Auranofin/Vitamin C: A Novel Drug Combination Targeting Triple-Negative Breast Cancer

Elie Hatem, Sandy Azzi, Nadine El Banna, Tiantian He, Amélie Heneman-Masurel, Laurence Vernis, Dorothée Baïlle, Vanessa Masson, Florent Dingli, Damarys Loew, et al.

JNCI 17-1468R2

Article

Auranofin/vitamin C: a novel drug combination targeting triple-negative breast cancer

Elie Hatem[1], Sandy Azzi[2], Nadine El Banna[1], Tiantian He[1], Amélie Heneman-Masurel[1], Laurence Vernis[1], Dorothée Baïlle[1], Vanessa Masson[3], Florent Dingli[3], Damarys Loew[3], Bruno Azzarone[4], Pierre Eid[2], Giuseppe Baldacci[5], Meng-Er Huang[1*]

[1] Institut Curie, PSL Research University, CNRS UMR3348, Université Paris-Sud, Université Paris-Saclay, 91405 Orsay, France.

[2] INSERM U1197, Hôpital Paul Brousse, Villejuif, France.

[3] Institut Curie, Centre de Recherche, PSL Research University, Laboratoire de Spectrométrie de Masse Protéomique, Paris, France.

[4] Immunology Research Area, IRCCS, Ospedale Bambino Gesù, Rome, Italy.

[5] Institut Jacques Monod, CNRS-Université Paris Diderot, Paris, France.

Running title: Targeting cancer cells with redox-based mechanisms

Keywords: auranofin, vitamin C, PTGR1, oxidative stress, redox modulation, triple-negative breast cancer, cancer.

*Correspondence to:

Meng-Er Huang, CNRS UMR3348, Institut Curie, Bâtiment 110, Centre Universitaire, 91405 Orsay, France. Phone: 33-1-69863016; Fax: 33-1-69869429; e-mail: meng-er.huang@curie.fr

Abstract

Background: Cancer cells from different origins exhibit various basal redox status and thus respond differently to intrinsic or extrinsic oxidative stress. These intricate characteristics condition the success of redox-based anticancer therapies that capitalize on the ability of reactive oxygen species to achieve selective and efficient cancer cell killing.

Methods: Redox biology methods, SILAC (stable isotope labeling by amino acids in cell culture)-based proteomics and bioinformatics pattern comparisons were used to decipher the underlying mechanisms for differential response of lung and breast cancer cell models to redox-modulating molecule auranofin (AUF) and to combinations of AUF and vitamin C (VC). The in vivo effect of AUF, VC, and two AUF/VC combinations on mice bearing MDA-MB-231 xenografts (n = 5 mice per group) was also evaluated. All statistical tests were two-sided.

Results: AUF targeted simultaneously the thioredoxin and glutathione antioxidant systems. AUF/VC combinations exerted a synergistic and hydrogen peroxide (H_2O_2)-mediated cytotoxicity towards MDA-MB-231 cells and other breast cancer cell lines. The anticancer potential of AUF/VC combinations was validated in vivo on MDA-MB-231 xenografts in mice without notable side effects. On day 14 of treatments, mean tumor volumes for vehicle-treated control group and the two AUF/VC combinations-treated groups (A/V1 and A/V2) were 197.67 ± 24.28, 15.66 ± 10.90 and 10.23 ± 7.30 mm^3 respectively, adjusted *P* values of the differences between mean tumor volumes of vehicle vs A/V1 groups and vehicle vs A/V2 groups were both less than .001. SILAC proteomics, bioinformatics analysis, and functional experiments linked prostaglandin reductase 1 (PTGR1) expression levels with breast cancer cell sensitivity to AUF/VC combinations.

Conclusion: Combination of AUF and VC, two commonly available drugs, could be efficient against triple-negative breast cancer and potentially other cancers with similar redox properties and PTGR1 expression levels. Redox-based anticancer activity of this combination and the discriminatory potential of PTGR1 expression are worth further assessment in preclinical and clinical studies.

Introduction

The difference in intrinsic reactive oxygen species (ROS) levels and redox status between normal and malignant cells provides a potential window to develop redox-based therapeutic approaches (1, 2). Despite sharing common hallmarks (3, 4), cancer cells from different origins exhibit different basal redox status and react differently to further intrinsic or extrinsic oxidative stress. These intricate characteristics condition cancer cell sensitivity to redox-modulating anticancer molecules or even to standard chemotherapeutic drugs that, in many cases, induce oxidative stress (5, 6).

Auranofin (AUF) is an oral gold-containing drug initially approved by the U.S. Food and Drug Administration for treatment of rheumatoid arthritis. AUF targets thioredoxin reductase (TRXR) and was recently repurposed as a potent anticancer drug (7-10). AUF is currently in clinical trials for chronic lymphocytic leukemia, ovarian cancer and lung cancer (https://clinicaltrials.gov/ct2/show/NCT01419691, NCT01747798, NCT01737502). However, cellular response to AUF varies considerably (11, 12).

In this study, we used lung and breast cancer cell models to decipher the factors that condition cancer cell response to AUF. We demonstrated that the anticancer activity of AUF relies on impacting both the glutathione and thioredoxin systems. Importantly, we discovered that AUF and L-ascorbic acid (vitamin C, VC) combinations exert a synergistic and hydrogen peroxide (H_2O_2)-mediated cytotoxicity towards triple-negative breast cancer (TNBC) cell lines, which was further validated in vivo in mice bearing MDA-MB-231 xenografts. We showed that prostaglandin reductase 1 (PTGR1) expression levels are linked with cellular sensitivity to AUF/VC combinations, suggesting the use of PTGR1 as a potential predictive biomarker.

Methods

All experimental materials and methods are detailed in the **Supplementary Methods**.

Cell Lines and Drugs

A549 (non-small-cell lung carcinoma cells), MDA-MB-231 (TNBC cells), HUVEC (human umbilical vein endothelial cells) and human dermal fibroblasts were purchased from American Type Culture Collection (Manassas, Virginia). HMEC (human mammary epithelial cells) were from Lonza (Basel, Switzerland). Additional breast cancer cell lines are described in the **Supplementary Methods**. AUF and VC were purchased from Enzo Life Sciences (Farmingdale, New York) and Sigma-Aldrich (Saint Louis, Missouri), respectively.

Evaluation of Cell Viability in Vitro

Cells were seeded in 96-well plates at a density of 1.25×10^4 cells per well for 24 hours and subjected to treatments. Cellular viability was assessed using the MTT (3-[4,5-dimethylthiazol-2-yl]-2,5-diphenyltetrazolium bromide) assay (Thermo Fisher Scientific, Waltham, Massachusetts). For colony formation assay, cells treated with defined conditions were further cultured for 10 to 12 days. Colonies were stained with 0.5% crystal violet solution and counted using ImageJ software (NIH, Bethesda, Maryland). Flow cytometry-based cell death assessment was performed using annexin V-FITC/propidium iodide (PI) staining (Thermo Fisher Scientific) and were analyzed using FlowJo software (FlowJo LLC, Ashland, Oregon). Data of combined drug effects were analyzed by the Chou and Talalay method using CompuSyn software (13). Combination index values of less than 1, 1, and more than 1 indicated synergism, additive effect, and antagonism, respectively.

SILAC (Stable Isotope Labeling by Amino Acids in Cell Culture)-based Mass Spectrometry Analysis

Standard SILAC medium preparation and labeling steps were performed according to the manufacturer (Thermo Fisher Scientific). Proteins from A549 and MDA-MB-231 cells were extracted and analyzed by nano-LC-MS/MS. Data were acquired using the Xcalibur software (v 3.0) (Thermo Fisher Scientific) and the resulting spectra were interrogated by Sequest HT through Thermo Scientific Proteome Discoverer (v 2.1) with the SwissProt Homo Sapiens database (012016). Experiment details are presented in the **Supplementary Methods**.

Mouse Experiments

Mouse experiments were reviewed and approved by the ethical committee CAPSUD/N°26 (reference number: 3898/2016020310283077). MDA-MB-231 cells were injected subcutaneously into the left and right flanks of 7-week-old female Swiss Nude Mice Crl:NU(Ico)-Foxn1^{nu} (Charles River laboratories, Wilmington, Massachusetts). Mice with tumors of 40–60 mm^3 were randomly assigned into five groups, each containing five mice. Mice were treated once a day by intraperitoneal injection (except Saturday and Sunday) for 15 days with phosphate-buffered saline (PBS, vehicle), AUF 10 mg/kg, VC 4 g/kg, AUF 5 mg/kg + VC 4 g/kg (designated A/V1) or AUF 10 mg/kg + VC 4 g/kg (designated A/V2). Tumor sizes were measured with electronic calipers. Experiment details are presented in the **Supplementary Methods**.

Statistical Analysis

Statistical significance of each data set was analyzed by one-way, two-way ANOVA or t test, as appropriate. Dose-response modeling, half maximal inhibitory concentration (IC50) calculations, and Spearman's correlation analyses were also performed. All statistical tests were two-sided. *P* values and adjusted *P* values less than .05 were considered statistically

significant.GraphPad Prism 7 software (GraphPad Software Inc., California) was used for calculating these statistics.

Results

Sensitivity of A549 and MDA-MB-231 Cells to AUF

A549 and MDA-MB-231 cells were treated with AUF ranging from 0.3 to 6 µM for 24 hours. MTT assays revealed that 6 µM AUF killed totally the MDA-MB-231 cells (mean viability ± SD = 0.51 ± 1.22%, adjusted $P < .001$), while having moderate effect on A549 cells (mean viability ± SD = 72.78 ± 12.64%, adjusted $P < .001$) (**Figure 1A**). Annexin/PI staining suggested a non-apoptotic cell death (**Supplementary Figure 1A**). IC50 of AUF for A549 and MDA-MB-231 was 7.59 µM and 2.34 µM respectively. Treatment with 6 µM AUF for 4 hours totally inhibited colony formation of MDA-MB-231 cells, while reduced only by 50% colony number of A549 cells (**Figure 1B**), confirming higher sensitivity of MDA-MB-231 cells to AUF, although its intrinsic lower baseline colony formation capacity should be taken into account (**Figure 1B**).

Given these observations, 6 µM AUF was further used as reference concentration to evaluate early impact of AUF on the redox systems. Basal TRXR activity was higher in A549 than in MDA-MB-231 cells, nevertheless, 6 µM AUF for 1 hour statistically significantly inhibited TRXR activity in both cell lines (adjusted $P < .001$) (**Figure 1C**). Under this condition, partial and total oxidation of peroxiredoxin 1 (PRDX1) and mitochondria-localized peroxiredoxin 3 (PRDX3) respectively were observed in MDA-MB-231 cells (**Figure 1D**), in contrast to moderate PRDX3 oxidation in A549 cells. Thus, AUF mainly impacted PRDX3, in accordance with an earlier report (14). Furthermore, 6 µM AUF caused ROS accumulation

in MDA-MB-231 but not in A549 cells (**Figure 1E**). These data suggest that A549 cells have a stronger antioxidant capacity than MDA-MB-231, promoting resistance to AUF.

Implication of Glutathione in AUF-induced Cell Death

Elevated intracellular glutathione usually correlates with resistance to pro-oxidants (15). Indeed, A549 exhibited an elevated basal level of glutathione compared with MDA-MB-231 cells (adjusted $P < .001$) and a higher resistance to AUF-induced glutathione depletion (**Figure 2A**). However, treatment of A549 cells with elevated AUF concentrations (10 and 12 μM) caused glutathione depletion (**Figure 2B**), statistically significant cell death (adjusted $P < .001$) (**Figure 2C**) and PRDX1 and PRDX3 oxidation (**Figure 2D**). DNCB (1-chloro-2,4-dinitrobenzene) is a TRXR inhibitor and an inducer of glutathione depletion (16). Treatment of A549 cells with DNCB (up to 80 μM) alone for 30 min mildly affected viability (**Figure 2E**), depleted glutathione ($P = .003$) (**Figure 2F**), inhibited TRXR activity (adjusted $P < .001$) (**Figure 2G**) and increased general ROS levels (adjusted $P < .001$) (**Figure 2H**). In contrast, treatment with DNCB for 30 min followed by 6 μM AUF for additional 24 hours efficiently killed A549 cells (adjusted $P < .001$) (**Figure 2E**), further decreased TRXR activity (adjusted $P = .009$) (**Figure 2G**) and further increased general ROS levels (adjusted $P < .001$) (**Figure 2H**). On the other hand, reduced glutathione (GSH) or N-acetyl-L-cysteine (NAC) but not oxidized glutathione (GSSG) suppressed AUF-induced MDA-MB-231 cell death (adjusted $P < .001$) without restoring TRXR activity (**Figure 2I, J**). These data indicate that, in addition to inhibiting TRXR activity, AUF depletes glutathione in a dose-dependent manner, leading to ROS accumulation and cell death.

Anticancer Effect of AUF/VC Combination

The results described above indicate that AUF is an efficient redox modulator and can be used to sensitize cancer cells to ROS-mediated challenges. Indeed, rational combinations of AUF and vitamin C (VC), a ROS generator and redox modulator (17-20), exerted synergistic cytotoxicity towards MDA-MB-231 cells, with combination index values less than 1 (**Figure 3A**). AUF 1 µM combined with VC 2.5 mM, specifically designated AUF-VC to distinguish from other AUF/VC combinations throughout the manuscript, was an optimal combination that preferentially killed MDA-MB-231 cells (adjusted $P < .001$) with much less impact on non-cancerous cell lines HMEC, human dermal fibroblasts and HUVEC (**Figure 3B**). The AUF-VC had a moderate toxicity on HMEC and minor or no effect on human dermal fibroblasts and HUVEC. Indeed, HUVEC colony formation capacity was not affected by the AUF-VC comparing with 6 µM AUF (**Figure 3D**), highlighting the advantage of using an AUF/VC combination over high-dose AUF. A549 cells were resistant to AUF-VC (**Figure 3B, C**). As for AUF alone, the AUF-VC induced non-apoptotic cell death in MDA-MB-231 cells (**Supplementary Figure 1B**).

Proteome Comparison: A549 versus MDA-MB-231

In order to understand the mechanistic basis of this different sensitivity between A549 and MDA-MB-231 cells to AUF and the AUF-VC, their proteomes were compared using quantitative SILAC-based analysis. 4131 proteins common to both cell lines were quantified among which 413 presented an absolute fold change in expression level ≥ 2 with an adjusted *P* value ≤ .05 (**Supplementary Table 1**). Of note, proteins involved in glutathione synthesis and reduction and in the pentose phosphate pathway (PPP) were more abundant in A549 cells, PPP being a key pathway generating NADPH, the main electron source for both the thioredoxin and the glutathione systems (21, 22). Furthermore, proteins belonging to other

metabolic pathways including AGR2 (63.5-fold), AK1BA (36.8-fold), PGDH (31.5-fold) and PTGR1 (12.2-fold) were also highly abundant in A549 cells.

To identify which of the 413 differently expressed proteins may correlate with cellular response to AUF/VC combinations, we performed pattern comparisons for AUF and VC anticancer activities using NCI-60 CellMiner web tool (23, 24). Gene transcript levels corresponding to 69 proteins exhibited a statistically significant correlation with AUF activity, 54 genes correlated negatively while 15 positively. On the other hand, expression levels of 26 genes statistically significantly correlated with VC activity, among which 17 correlated negatively while 9 positively. We thus generated a list of 17 genes with 12 correlating negatively and 5 positively with both AUF and VC effect (**Table 1**). Among these 17 genes, *PTGR1* exhibited the highest statistically significant Pearson's correlation values for both AUF and VC ($r = -0.538$ and -0.608, $P = 9.70\times10^{-5}$ and 0, respectively), which suggests its potential use as a predictive biomarker for cancer cell response to AUF/VC combinations.

Correlation between PTGR1 Expression and Cellular Response to AUF/VC Combinations

We queried the *PTGR1* gene expression data of 34 breast cancer cell lines of the Curie Institute collection. The majority (85.3%) displayed lower *PTGR1* mRNA levels compared with MDA-MB-231 (**Figure 4A**). We first chose a panel of five TNBC cell lines with different PTGR1 mRNA levels, including MDA-MB-231 (*PTGR1* mRNA expression = 9.11), HCC-1937 (8.76), BT-549 (8.24), MDA-MB-468 (7.24) and HCC-1187 (6.28). TNBC represents a heterogeneous and aggressive breast cancer subtype with a poor prognosis (27, 28). Western blot showed a consistent pattern between PTGR1 mRNA and protein levels (**Figure 4A, B**). These five TNBC cell lines were all sensitive to the AUF-VC (**Figure 4C**). We determined the IC50 of AUF/VC combination for each cell line and found that cells with

higher PTGR1 expression were more resistance to AUF/VC combination (**Figure 4D**, **Supplementary Figure 2**). HCC-1187 cells exhibiting the lowest PTGR1 expression had the highest sensitivity to AUF/VC combination.

The link between PTGR1 expression levels and cellular response to AUF/VC combination was validated by PTGR1 knockdown or overexpression experiments. PTGR1 silencing rendered MDA-MB-231 cells more sensitive to AUF/VC combinations (adjusted $P < .001$) (**Figure 4E**), and even sensitized highly resistant A549 cells (**Figure 4F**). On the other hand, PTGR1 overexpression in HCC-1187 cells enhanced *per se* cellular growth (adjusted $P = .04$) and conferred resistance to AUF/VC treatment (adjusted $P < .001$) (**Figure 4G**).

To address whether this link can be true for breast cancer in general, we included to the study five non-TNBC breast cancer cell lines exhibiting different *PTGR1* mRNA expression levels (**Figure 4A**) (26). Their IC50 values were close to those of TNBC cell lines (**Supplementary Figure 2**), indicating that AUF/VC combination may be effective for non-TNBC cells as well. With this panel of 10 cell lines, Spearman's correlation and linear regression analysis showed a moderate but statistically significant correlation between PTGR1 expression and AUF/VC response (Spearman's $r = 0.649$, $P = .049$) (**Figure 4H**). The tendency of correlation appeared to be more pronounced in TNBC cell lines. Consistently, PTGR1 knockdown in HCC-1954 cells, an HER2-positive breast cancer cell line, conferred a higher sensitivity to AUF/VC combinations (**Figure 4I**), but yet a mild effect when compared with that observed in MDA-MB-231 cells (**Figure 5E**). A larger set of breast cancer cell lines is required to achieve a statistically sound conclusion for each breast cancer subtype.

To further address whether the existence and degree of correlation between PTGR1 expression and cancer response to AUF/VC combinations may vary among cancer cell types or subtypes, we retrieved *PTGR1* mRNA expression data of 60 cancer cell lines of different

origins as well as their sensitivity to AUF or VC from NCI-60 database (**Supplementary Figure 3A**). The small number of cell lines in each cancer type prevented a statistically sound correlation analysis. Nevertheless, most of PTGR1-overexpressing lung cancer cell lines showed resistance to AUF and VC, the only cell line with low PTGR1 levels (NCI-H522) was sensitive to both drugs (**Supplementary Figure 3B, C**). Interestingly, the enhanced toxicity of AUF/VC combinations on PTGR1-silenced A549 cells was consistent with this prediction (**Figure 4F**). Taken together, our data and bioinformatics analyses indicate that the link between PTGR1 expression and cancer cell sensitivity to AUF/VC combination may be valid for specific cancer types or subtypes.

Reactive Species Responsible for the AUF-VC Induced Cytotoxicity

Treatment with the AUF-VC for 2 hours led to a statistically significant increase in ROS level in MDA-MB-231 cells (adjusted $P < .001$) (**Figure 5A**). The presence of 2 mM GSH or polyethylene glycol-catalase (PEG-CAT, 500 and 2000 U/ml) suppressed the AUF-VC induced cell death, while polyethylene glycol-superoxide dismutase (PEG-SOD) showed no protective effect (**Figure 5B**). Consistently, the treatment with the AUF-VC, but not AUF or VC alone, induced a statistically significant oxidation of H_2O_2-specific HyPer sensors (29) targeted to cytosol, nucleus or mitochondrial matrix of MDA-MB-231 cells (adjusted $P < .001$) (**Figure 5C**). This effect was abrogated by the presence of PEG-CAT. The sum of these results indicates that H_2O_2 is the main reactive species responsible for the AUF-VC induced toxicity.

Effect of AUF/VC Combinational Treatment in Vivo

VC and AUF represent clinically interesting and applicable compounds (7, 30). Our in vitro data on TNBC cell lines prompted us to explore the effect of AUF/VC combination in vivo.

Mice bearing MDA-MB-231 xenografts were treated with PBS (vehicle), AUF 10 mg/kg, VC 4 g/kg, AUF 5 mg/kg + VC 4 g/kg (A/V1) or AUF 10 mg/kg + VC 4 g/kg (A/V2). All treatment regimens were well tolerated as indicated by an absence of weight loss (**Figure 6A**) or blood count anomalies (Figure 6B) or liver or kidney necrosis (**Supplementary Figure 4**). Remarkably, the treatment with either A/V1 or A/V2 induced statistically significant tumor regression within 15 days of treatment. At this time point, mean tumor volumes for vehicle, A/V1 and A/V2 groups were 197.67 ± 24.28, 15.66 ± 10.90 and 10.23 ± 7.30 mm^3 respectively, adjusted *P* values of the differences between tumor volumes of vehicle vs A/V1 and vehicle vs A/V2 were both less than .001 (**Figure 6C, D**), while tumor growth in vehicle-treated, AUF-treated, and VC-treated groups was similar. Exponential and linear fit of tumor growth curves confirmed an inhibition of tumor growth in A/V1 and A/V2 groups (**Supplementary Figure 5**). Hematoxylin and eosin staining of biopsy of the remaining tumors indicated that AUF/VC combinations caused massive necrotic cell death (**Figure 6E**). These data confirmed our in vitro findings, demonstrating that tumor derived from a representative TNBC cell line can be suppressed efficiently in vivo using AUF/VC combinations without obvious side effects.

Discussion

AUF is known to be a specific TRXR inhibitor and has received increasing attention as a potential anticancer drug (7-10, 14). In this study, we demonstrated that the anticancer activity of AUF relies on impacting both the glutathione and thioredoxin systems. Cell death occurs at doses where AUF concomitantly depletes glutathione and inhibits thioredoxin system, in accordance with the complex interplay and compensatory role between the glutathione and thioredoxin systems (22, 31).

VC, at high concentrations, becomes a ROS-generating and redox-modulating molecule (17-20). We discovered that AUF and VC combinations produce a synergistic and selective anticancer effect on breast cancer cells in vitro. AUF 1 µM combined with VC 2.5 mM (AUF-VC) was as toxic as 6 µM AUF towards MDA-MB-231 cells but was safe to some extent for normal cells unlike 6 µM AUF. These findings are potentially clinically relevant since plasma AUF concentrations of approximately 1~3 µM are achievable with tolerable side effects in patients or volunteer subjects who received the recommended dose for rheumatoid arthritis, typically 6 mg/day (32, 33). Whether higher plasma AUF concentrations could be readily achieved and tolerable are unknown. We predict that beyond 3 µM, AUF may exert more severe adverse side effects as suggested by the toxicity of 6 µM AUF on HUVEC observed in vitro. On the other hand, plasma VC concentrations greater than 10 mM are achievable in humans and are well tolerated (30). Therefore, AUF/VC combination should increase anticancer efficacy, and decrease dosage and side effects of single drugs. This is validated in mice bearing MDA-MB-231 xenografts where AUF/VC combinations revealed higher therapeutic efficacy than single drugs.

The reasons underlying the different sensitivity observed between A549 and MDA-MB-231 cells to AUF and to AUF/VC combination could be multifactorial. Of note, NRF2, the key transcriptional regulator of antioxidant systems, is constitutively stabilized in A549 cells (34, 35). The sustained induction of NRF2-targeted genes and NRF2-dependent metabolic reprogramming that favors NADPH production, confirmed in our SILAC-based proteome comparison between A549 and MDA-MB-231 cells, could explain the low ROS levels in A549 cells and their resistance to AUF and AUF/VC combination. Interestingly, *PTGR1* expression levels that were found high in A549 cells are also regulated by NRF2 (36). PTGR1 exerts a protective effect against H_2O_2- and 4-hydroxynonenal-induced cell death

(36). Therefore, PTGR1 may play such role against H_2O_2 generated by AUF/VC combinations, conferring resistance.

Limitations of our study should be considered. The therapeutic efficacy of AUF/VC combinations needs to be ascertained using a larger set of mouse TNBC cell line and patient-derived xenografts. Similarly, the absence of side effects of AUF/VC combinations were investigated in the mouse models over a short period of time (two weeks), but long-term treatments and subsequent clinical trials are needed to confirm the safety of this new drug combination. Finally, whether PTGR1 could be used as an effective biomarker for response of TNBC, breast cancer in general, or even other cancer types or subtypes to AUF/VC combinations also requires extended studies, using a larger set of cell lines and clinical data. It is worth noting that in our study, low PTGR1 expression tends to correlate with increased cellular sensitivity to AUF/VC combination. This is in contrast with an earlier report demonstrating that PTGR1 induction enhances cellular sensitivity to hydroxymethylacylfulvene, a drug used for the treatment of advanced solid tumors (37). Thus, modulation of one gene may have opposite functional impact and different predictive value depending on the type of cancer, the drug used, and its mechanism of action.

In summary, this study shows that a combination of two non-toxic and commonly available drugs, AUF and VC, could be efficient against TNBC and potentially other cancers with similar redox properties. PTGR1 can be considered as a potential biomarker at least for TNBC cell lines and its use to select cancer patients who will mostly respond to AUF/VC combination should be further evaluated.

Funding

This work was supported by the CNRS, the Institut Curie, the Institut National du Cancer SiRIC grant (INCa-DGOS-4645 to M.-E.H), la Fondation ARC grant (PJA 20151203330 to

M.-E.H). E. Hatem is supported by a postdoctoral fellowship from the Ligue Nationale Contre le Cancer and Crédit Agricole île de France Mécénat, N. El Banna is supported by PhD program from the Université Paris-Saclay.

Notes

The funders had no role in design of the study, the collections, analysis, or interpretation of the data, the writing of the manuscript, or the decision to submit the manuscript for publication.

We thank Sergio Roman Roman, Mounira Amor-Guéret, Stéphan Vagner, Jean-Michel Camadro, Thibaut Léger and Camille Garcia for helpful discussions. We also thank Alice Pinheiro and Fabien Reyal for providing cell lines, Carsten Janke and Puja Singh for providing reagents, Charlène Lasgi, Marie-Noëlle Soler, Guillaume Arras and Bérangère Lombard for technical and bioinformatics assistance, and Etienne Thevenot for advice on statistical analysis.

Author contributions: EH and MEH conceived and designed the project. EH, SA, NEB, TH, AHM, LV, DB, VM, FD, DL and MEH performed experiments. EH, SA, NEB, DL, BA, PE, GB and MEH analyzed and interpreted the data. EH and MEH wrote the manuscript with input from SA, NEB, LV, DL, BA, PE and GB. All authors contributed to the review, revision and approval of the final manuscript.

The authors declare no conflicts of interests.

References

1. Trachootham D, Alexandre J, Huang P. Targeting cancer cells by ROS-mediated mechanisms: a radical therapeutic approach? *Nat Rev Drug Discov.* 2009; 8 (7):579-591.

2. Gorrini C, Harris IS, Mak TW. Modulation of oxidative stress as an anticancer strategy. *Nat Rev Drug Discov.* 2013; 12(2):931-947.

3. Hanahan D, Weinberg RA. Hallmarks of cancer: the next generation. *Cell.* 2011; 144(5):646-674.

4. Pavlova NN, Thompson CB. The emerging hallmarks of cancer metabolism. *Cell Metab.* 2016; 23(1):27-47.

5. Conklin KA. Chemotherapy-associated oxidative stress: impact on chemotherapeutic effectiveness. *Integr Cancer Ther.* 2004; 3(4):294-300.

6. Rana T, Chakrabarti A, Freeman M, Biswas S. Doxorubicin-mediated bone loss in breast cancer bone metastases is driven by an interplay between oxidative stress and induction of TGFbeta. *PloS one* 2013; 8:e78043.

7. Roder C, Thomson MJ. Auranofin: repurposing an old drug for a golden new age. *Drugs R D.* 2015; 15(1):13-20.

8. Fiskus W, Saba N, Shen M, et al. Auranofin induces lethal oxidative and endoplasmic reticulum stress and exerts potent preclinical activity against chronic lymphocytic leukemia. *Cancer Res.* 2014; 74(9):2520-2532.

9. Topkas E, Cai N, Cumming A, et al. Auranofin is a potent suppressor of osteosarcoma metastasis. *Oncotarget.* 2016; 7(1):831-844.

10. Wang H, Bouzakoura S, de Mey S, et al. Auranofin radiosensitizes tumor cells through targeting thioredoxin reductase and resulting overproduction of reactive oxygen species. *Oncotarget*. 2017; 8(22):35728-35742.

11. Kim NH, Park HJ, Oh MK, Kim IS. Antiproliferative effect of gold(I) compound auranofin through inhibition of STAT3 and telomerase activity in MDA-MB 231 human breast cancer cells. *BMB Rep.* 2013; 46(1):59-64.

12. Fan C, Zheng W, Fu X, Li X, Wong YS, Chen T. Enhancement of auranofin-induced lung cancer cell apoptosis by selenocystine, a natural inhibitor of TrxR1 in vitro and in vivo. *Cell Death Dis.* 2014; 5:e1191.

13. Chou TC. Drug combination studies and their synergy quantification using the Chou-Talalay method. *Cancer Res.* 2010; 70(2):440-446.

14. Gandin V, Fernandes AP, Rigobello MP, et al. Cancer cell death induced by phosphine gold(I) compounds targeting thioredoxin reductase. *Biochem Pharmacol.* 2010; 79(2):90-101.

15. Hatem E, El Banna N, Huang ME. Multifaceted roles of glutathione and glutathione-based systems in carcinogenesis and anticancer drug resistance. *Antioxid Redox Signal.* 2017; 273(15):1217-1234.

16. Nordberg J, Zhong L, Holmgren A, Arner ES. Mammalian thioredoxin reductase is irreversibly inhibited by dinitrohalobenzenes by alkylation of both the redox active selenocysteine and its neighboring cysteine residue. *J Biol Chem.* 1998; 273(18):10835-10842.

17. Yun J, Mullarky E, Lu C, et al. Vitamin C selectively kills KRAS and BRAF mutant colorectal cancer cells by targeting GAPDH. *Science.* 2015; 350(6266):1391-1396.

18. Chen Q, Espey MG, Krishna MC, et al. Pharmacologic ascorbic acid concentrations selectively kill cancer cells: action as a pro-drug to deliver hydrogen peroxide to tissues. *Proc Natl Acad Sci U S A.* 2015; 102(38):13604-13609.

19. Schoenfeld JD, Sibenaller ZA, Mapuskar KA, et al. $O_2^{\bullet-}$ and H_2O_2-mediated disruption of Fe metabolism causes the differential susceptibility of NSCLC and GBM cancer cells to pharmacological ascorbate. *Cancer cell.* 2017; 31 (4):487-500.

20. Du J, Cullen JJ, Buettner GR. Ascorbic acid: chemistry, biology and the treatment of cancer. *Biochim Biophys Acta.* 2012; 1826 (2):443-457.

21. Patra KC, Hay N. The pentose phosphate pathway and cancer. *Trends Biochem Sci.* 2014; 39 (8):347-354.

22. Lu J, Holmgren A. The thioredoxin antioxidant system. *Free Radic Biol Med.* 2014; 66:75-87.

23. Reinhold WC, Sunshine M, Liu H, et al. CellMiner: a web-based suite of genomic and pharmacologic tools to explore transcript and drug patterns in the NCI-60 cell line set. *Cancer Res.* 2012; 72(14), 3499-3511.

24. Reinhold WC, Sunshine M, Varma S, Doroshow JH, Pommier Y. Using CellMiner 1.6 for systems pharmacology and genomic analysis of the NCI-60. *Clin Cancer Res.* 2015; 21(17):3841-3852.

25. Ritchie ME, Phipson B, Wu D, et al. limma powers differential expression analyses for RNA-sequencing and microarray studies. *Nucleic Acids Res.* 2015; 43(7):e47.

26. Benjamini Y, Hochberg Y. Controlling the false discovery rate: a practical and powerful approach to multiple testing. *J R Statist Soc B.* 1995; 57(1):289-300.

27. Bianchini G, Balko JM, Mayer IA, Sanders ME, Gianni L. Triple-negative breast cancer: challenges and opportunities of a heterogeneous disease. *Nat Rev Clin Oncol.* 2016; 13 (11):674-690.

28. Neve RM, Chin K, Fridlyand J, et al. A collection of breast cancer cell lines for the study of functionally distinct cancer subtypes. *Cancer Cell.* 2006; 10 (6):515-527.

29. Belousov VV, Fradkov AF, Lukyanov KA, et al. Genetically encoded fluorescent indicator for intracellular hydrogen peroxide. *Nat Methods*. 2006; 3(4):281-286.

30. Stephenson CM, Levin RD, Spector T, Lis CG. Phase I clinical trial to evaluate the safety, tolerability, and pharmacokinetics of high-dose intravenous ascorbic acid in patients with advanced cancer. *Cancer Chemother Pharmacol.* 2013; 72(1):139-146.

31. Harris IS, Treloar AE, Inoue S, et al. Glutathione and thioredoxin antioxidant pathways synergize to drive cancer initiation and progression. *Cancer Cell*. 2015; 27 (2):211-222.

32. Capparelli EV, Bricker-Ford R, Rogers MJ, McKerrow JH, Reed SL. Phase I clinical trial results of auranofin, a novel antiparasitic agent. *Antimicrob Agents Chemother*. 2016; 61(1):e01947-16.

33. Van Riel PL, Gribnau FW, Van de Putte LB, et al. Serum gold concentrations during treatment with auranofin. *Clin Rheumatol.* 1987; 6 (1):50-54.

34. Jaramillo MC, Zhang DD. The emerging role of the Nrf2-Keap1 signaling pathway in cancer. *Genes Dev*. 2013; 27(20):2179-2191.

35. Menegon S, Columbano A, Giordano S. The dual roles of NRF2 in cancer. *Trends Mol Med.* 2016; 22(7):578-593.

36. Sanchez-Rodriguez R, Torres-Mena JE, Quintanar-Jurado V, et al. Ptgr1 expression is regulated by NRF2 in rat hepatocarcinogenesis and promotes cell proliferation and resistance to oxidative stress. *Free Radic Biol Med*. 2017; 102:87-99

37. Yu X, Erzinger MM, Pietsch KE, et al. Up-regulation of human prostaglandin reductase 1 improves the efficacy of hydroxymethylacylfulvene, an antitumor chemotherapeutic agent. *J Pharmacol Exp Ther*. 2012; 343(2):426-433.

Table 1. List of 17 genes with statistically significant Pearson correlations with both auranofin and vitamin C

Protein	Gene	SILAC: A549 /MDA-MB-231		Auranofin		Vitamin C	
		Ratio*	*P* value†	Gene transcript levels correlation coefficient‡	*P* value§	Gene transcript levels correlation coefficent‡	*P* value§
Increased							
TRXR1	*TXNRD1*	2.81	4.63×10^{-6}	-0.398	0.006	-0.401	0.002
ASPH	*ASPH*	5.35	3.29×10^{-7}	-0.530	1.26×10^{-4}	-0.369	0.004
HYEP	*EPHX1*	4.10	3.43×10^{-5}	-0.376	0.009	-0.456	2.84×10^{-4}
DSG2	*DSG2*	3.59	4.14×10^{-5}	-0.534	1.12×10^{-4}	-0.369	0.004
MYO1E	*MYO1E*	4.46	1.46×10^{-4}	-0.518	1.91×10^{-4}	-0.333	0.01
TRI16	*TRIM16*	4.75	3.66×10^{-5}	-0.497	3.83×10^{-4}	-0.455	2.98×10^{-4}
PTGR1	*PTGR1*	12.22	8.75×10^{-10}	-0.538	9.70×10^{-5}	-0.608	0.000
UGDH	*UGDH*	36.44	6.87×10^{-5}	-0.437	0.002	-0.357	0.005
AL3A2	*ALDH3A2*	10.31	0.01	-0.374	0.01	-0.350	0.007
Decreased							
CAV1	*CAV1*	0.26	0.002	-0.430	0.003	-0.360	0.005
ECE1	*ECE1*	0.16	0.002	-0.536	1.03×10^{-4}	-0.349	0.007
PP2BA	*PPP3CA*	0.24	0.02	-0.452	0.001	-0.355	0.006
LYAR	*LYAR*	0.42	1.31×10^{-4}	0.396	0.006	0.411	0.001
SRPK1	*SRPK1*	0.25	2.84×10^{-4}	0.379	0.009	0.427	7.42×10^{-4}
STMN1	*STMN1*	0.13	0.001	0.402	0.005	0.344	0.008
FKBP5	*FKBP5*	0.26	0.001	0.445	0.002	0.440	4.81×10^{-4}
CMTR1	*CMTR1*	0.28	0.045	0.479	6.68×10^{-4}	0.473	1.55×10^{-4}

* Ratio of protein levels between A549 and MDA-MB-231, obtained from SILAC data, are indicated and classified as "Increased" for the protein ratios ≥2 with $P < .05$, and "Decreased" for the protein ratios ≤ 0.5 with $P < .05$.

† *P* values were obtained by two-sided t test performed with the R package limma (25) adjusted with Benjamini-Hochberg procedure (26).

‡ Pearson correlations were generated from NCI-60 web tool (23, 24) (https://discover.nci.nih.gov/cellminer/home.do), Database Version 2.1. Pearson's correlation coefficients between gene transcript level and AUF or VC anticancer effect are indicated. Significant positive and negative correlations are identified at $r > 0.334$, $P < .05$, and $r < -0.334$, $P < .05$, respectively.

§ Two-sided *P* values were not adjusted for multiple comparisons and were generated from NCI-60 web tool.

Figure Legends

Figure 1. Sensitivity of A549 and MDA-MB-231 cells to AUF. A) A549 and MDA-MB-231 cells were treated with AUF at indicated concentrations for 24 hours and cell viability was measured with the MTT assay. Percent survival was calculated relative to non-treated cells. **B**) Colony formation of A549 and MDA-MB-231 cells after treatment with 6 µM AUF for 4 hours. Percent surviving fraction was calculated relative to non-treated cells. Representative images are presented. **C**) Total TRXR activity of cells with indicated treatments was measured using the Thioredoxin Reductase Assay Kit (Sigma-Aldrich). Values were normalized to the activity of 0.5 µg rat liver TRXR as a positive control (PC, set to 100%). The insert shows western blot of TRXR1 and TRXR2 of non-treated A549 and MDA-MB-231 cells. **D)** PRDX1 and PRDX3 redox states in cells treated with indicated conditions using redox western blot analysis. Graphs show the quantification of oxidized PRDX1 or PRDX3 form (%) versus total PRDX1 or PRDX3 protein. ox = oxidized, red = reduced. **E**) Flow cytometry-based ROS assessment using carboxy-H_2DCFDA in cells treated with indicated conditions. Mean fluorescence value in non-treated A549 cells is set as 1 and relative fluorescence intensity is represented. All statistical significance is assessed by two-way ANOVA with Sidak's or Tukey's multiple comparisons test. Sidak's correction is used for comparison between different cell lines while Tukey's for comparison of a given cell line treated with different conditions. Only part of statistical comparisons is indicated. Bar graphs show means ± SD of at least 3 independent experiments. NT = non-treated, A = A549, M = MDA-MB-231.

Figure 2. Implication of glutathione in AUF-induced cell death. A) Total intracellular glutathione levels of A549 and MDA-MB-231 cells treated with indicated conditions. Values

are reported as glutathione equivalents per µg of proteins. Two-sided *P* values were calculated by two-way ANOVA with Sidak's correction when different cell lines are compared, and Tukey's correction when comparing a given cell line treated with different conditions. **B**) Total intracellular glutathione levels of A549 cells treated with AUF for 3 hours at indicated concentrations. **C**) Viability of A549 cells treated with AUF at indicated concentrations for 24 hours was measured using the MTT assay. Percent survival was calculated relative to non-treated cells. **D**) PRDX1 and PRDX3 redox state of A549 cells treated with AUF at indicated concentrations. Graphs show the quantification of oxidized PRDX1 or PRDX (%) versus total PRDX1 or PRDX3 protein. ox = oxidized, red = reduced. **E**) A549 cells were treated with DNCB at indicated concentrations for 30 min followed by treatment with 6 µM AUF for 24 hours. Cell viability was measured using the MTT assay. **F**) Total intracellular glutathione level of A549 cells at indicated conditions. Values are reported as in (**A**). Two-sided *P* values were calculated by unpaired t test with Welch's correction. **G**) Total TRXR activity of A549 cells with or without DNCB treatment for 30 min followed by release for 1 hour in culture medium or an additional treatment with 6 µM AUF. Values were normalized to the activity of 0.5 µg rat liver TRXR as positive control (PC, set to 100%). **H**) Flow cytometry-based ROS assessment using carboxy-H_2DCFDA in non-treated A549 cells, cells treated with 40 µM DNCB for 30 min, and cells treated with 40 µM DNCB for 30 min followed by a treatment with 6 µM AUF for 1 hour. Mean fluorescence values of each condition were normalized to those of non-treated A549 (set as 1). **I**) MDA-MB-231 cells were treated with 6 µM AUF for 24 hours in the presence of NAC, GSH or GSSG at indicated concentrations. Cell viability was measured using the MTT assay. **J**) Total TRXR activity of MDA-MB-231 cells treated with or without 6 µM AUF for 1 and 24 hours in the presence of 2 mM GSH. Values are presented as in (**G**). One-way ANOVA with Tukey's multiple comparisons test was used to

calculate the two-sided values, except for Figure 2F. Bar graphs show means ± SD of at least 3 independent experiments.

Figure 3. Effect of AUF/VC combinations on cancer and normal cell lines. A) MDA-MB-231 cells were treated with AUF/VC combinations (AUF 1 µM/VC 1000 µM, AUF 1.5 µM/VC 1500 µM, AUF 2 µM/VC 2000 µM and AUF 3 µM/VC 3000 µM) for 24 hours. Cell viability was assessed using the MTT assay and fractional inhibition (100% – viability %) was derived. Combination index (CI) was calculated using CompuSyn software (13). Additive effect, CI = 1; synergism, CI < 1; antagonism, CI > 1. **B**) A549, MDA-MB-231, HMEC, normal human dermal fibroblasts and HUVEC were treated with 1 µM AUF combined with VC at indicated concentrations for 24 hours. Cell viability was measured using the MTT assay. Percent survival of each cell type was calculated relative to non-treated cells. Two-sided *P* values were calculated by two-way ANOVA with Sidak's multiple comparisons test. **C**) Colony formation of A549 and MDA-MB-231 cells after treatment with 1 µM AUF, 2.5 mM VC or the combination of 1 µM AUF and 2.5 mM VC (designated AUF-VC) for 24 hours. Representative images are presented. Percent surviving fraction was calculated relative to non-treated cells. Bar graphs show means ± SD of 3 independent experiments. Statistical difference in surviving fraction between cell lines or between different treatments for the same cell line is assessed by two-way ANOVA with Sidak's or Tukey's multiple comparisons test, respectively. **D**) Colony formation of HUVEC cells following treatment with 6 µM AUF or AUF-VC for 24 hours. *P* values were calculated using one-way ANOVA with Tukey's multiple comparisons test. All tests were two-sided.

Figure 4. PTGR1 expression and breast cancer cell response to AUF/VC combinations. A) *PTGR1* mRNA expression patterns in log2 values using transcriptomic datasets of the

Curie Institute breast cancer cell lines. Mean and median values are shown as solid and dashed lines, respectively. TNBC and non-TNBC cell lines used in this study are indicated in turquoise blue and orange respectively. **B)** Western blot analyses of PTGR1 expression in A549 and five TNBC cell lines. Statistical significance of the differences in PTGR1 protein levels is assessed by one-way ANOVA with Tukey's multiple comparisons test; all tests were two-sided. **C**) Viability of cells treated with the AUF-VC for 24 hours was measured using the MTT assay. Percent survival was calculated relative to non-treated cells (set to 100%). **D**) *PTGR1* mRNA expression (log2 values) from transcriptomic datasets of the Curie Institute (**A**) versus IC50 of AUF/VC combinations (log10 values) for five TNBC cell lines. **E**-**F**) MTT assay on MDA-MB-231 (**E**) and A549 (**F**) cells transfected with PTGR1 specific siRNA or control siRNA for 48 hours followed by treatments with 1 µM AUF combined with VC at indicated concentrations for 24 hours. The western blot insert shows siRNA-mediated PTGR1 knockdown. **G**) MTT assay on HCC-1187 cells transiently transfected with pCMV-based PTGR1 overexpression plasmid and pCMV control plasmids for 24 hours followed by treatments with AUF 1 µM /VC 1 mM for additional 24 hours. The western blot insert shows PTGR1 overexpression in transfected HCC-1187 cells. Two-sided P values were calculated by one-way ANOVA with Tukey's multiple comparisons test. **H**) Spearman's correlation and linear regression analysis regarding PTGR1 mRNA expression (log2 values) of 10 breast cell lines versus their IC50 for AUF/VC combinations (log10 values). PTGR1 mRNA expression was retrieved from transcriptomic datasets of the Curie Institute breast cancer cell lines. Different cell lines are indicated by symbols, the best-fit line is in red and the 95% confidence bands of the best-fit line are indicated in blue. Mathematical parameters are presented next to the graphs. **I**) MTT assay on HCC-1954 cells transiently transfected with PTGR1 siRNA or control siRNA for 48 hours followed by treatments with 1 µM AUF combined with VC at indicated concentrations for 24 hours. The western blot insert shows siRNA-mediated PTGR1

knockdown. All statistical tests were two-sided and *P* values were calculated by two-way ANOVA with Sidak's multiple comparisons test, except Figure 4B and 4G.

Figure 5. Reactive oxygen species responsible for the AUF/VC combination-induced cytotoxicity. A) ROS measurement in MDA-MB-231 cells treated with indicated conditions using carboxy-H2DCFDA. Mean fluorescence values of each condition were normalized to those of non-treated cells (set to 1). **B)** MTT assay on MDA-MB-231 cells treated with the AUF-VC for 24 hours in the presence of GSH, PEG-SOD, PEG-CAT. **C**) MDA-MB-231 cells expressing respectively cytosol-, nucleus-, and mitochondrial matrix-targeted HyPer were treated with indicated conditions for 2 hours. Treatment with 100 µM H_2O_2 for 30 min was used as a positive control (PC). HyPer redox state was evaluated by redox western blot. All bar graphs show means ± SD of at least 3 independent experiments. All tests were two-sided and *P* values were calculated by one-way ANOVA with Tukey's multiple comparisons test. NT = non-treated**.**

Figure 6. Anticancer effect of AUF/VC combinations on MDA-MB-231 xenografts in nude mice. A) Athymic nude female mice bearing MDA-MB-231 xenografts were treated, via intraperitoneal injection, with PBS (vehicle), AUF 10 mg/kg, VC 4 g/kg, AUF 5 mg/kg + VC 4 g/kg (A/V1) or AUF 10 mg/kg + VC 4 g/kg (A/V2). Mice from each group (5 mice per group) were weighed during the course of treatments and mean values ± SD are presented. **B**) At the end of treatments, blood samples of mice were obtained after cardiac puncture under anesthesia. Whole blood was analyzed using an automated hematology analyzer. WBC: whole blood cells, LYM: lymphocytes, MON: monocytes, NEU: neutrophils, RBC: red blood cells and MCV: mean corpuscular volume. **C**) Tumors sizes were measured two or three times per week. Mean tumor volume and SD are shown. **D**) Mean tumor volume ± SD of each group at

Day 0 (before treatment) and Day 14 (end of treatment) are presented. Statistical significance of the differences in mean tumor volumes between vehicle and indicated groups were determined by two-way ANOVA with Dunnett's multiple comparison test. **E**) Quantification of tumor necrosis (%) on tumor section following hematoxylin and eosin (H&E) staining using ImageJ software. All *P* values were calculated by one-way ANOVA with Tukey's multiple comparisons test and all tests were two-sided. Representative examples of necrotic area delimitation using ImageJ software on tumor sections of vehicle- and A/V2- treated mice are shown. Scale bar = 10 μm.

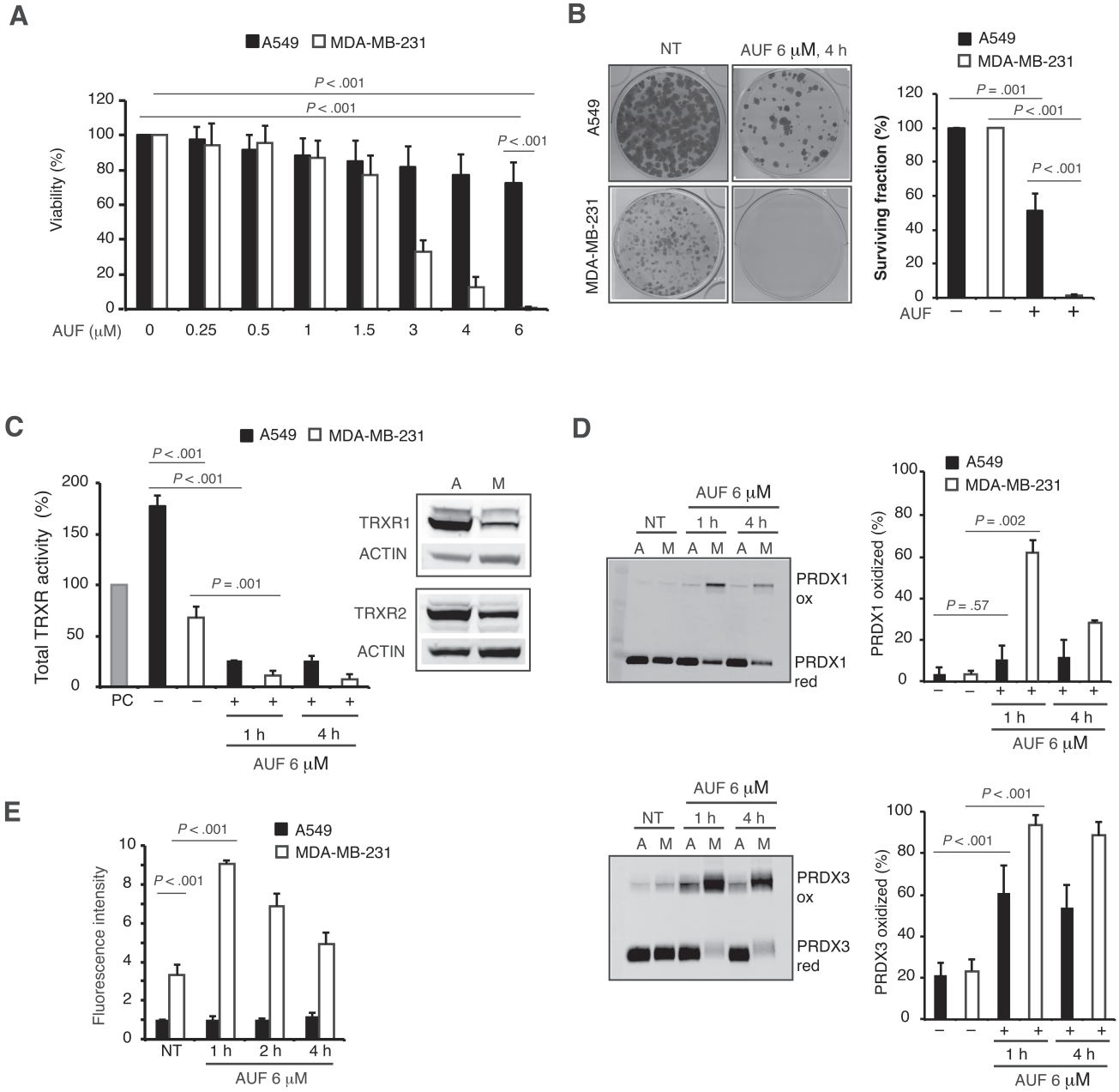
A
A549
MDA-MB-231
P < .001
P < .001
P < .001
Viability (%)
120
100
80
60
40
20
0
AUF (μM) 0 0.25 0.5 1 1.5 3 4 6
B
NT
AUF 6 μM, 4 h
A549
MDA-MB-231
A549
MDA-MB-231
P = .001
P < .001
P < .001
Surviving fraction (%)
120
100
80
60
40
20
0
AUF – – + +
C
A549
MDA-MB-231
P < .001
P < .001
P = .001
Total TRXR activity (%)
200
150
100
50
0
PC – – + + + +
1 h 4 h
AUF 6 μM
A M
TRXR1
ACTIN
TRXR2
ACTIN
D
AUF 6 μM
NT 1 h 4 h
A M A M A M
PRDX1 ox
PRDX1 red
A549
MDA-MB-231
P = .002
P = .57
PRDX1 oxidized (%)
100
80
60
40
20
0
– – + + + +
1 h 4 h
AUF 6 μM
AUF 6 μM
NT 1 h 4 h
A M A M A M
PRDX3 ox
PRDX3 red
P < .001
P < .001
PRDX3 oxidized (%)
100
80
60
40
20
0
– – + + + +
1 h 4 h
AUF 6 μM
E
P < .001
P < .001
A549
MDA-MB-231
Fluorescence intensity
10
8
6
4
2
0
NT 1 h 2 h 4 h
AUF 6 μM

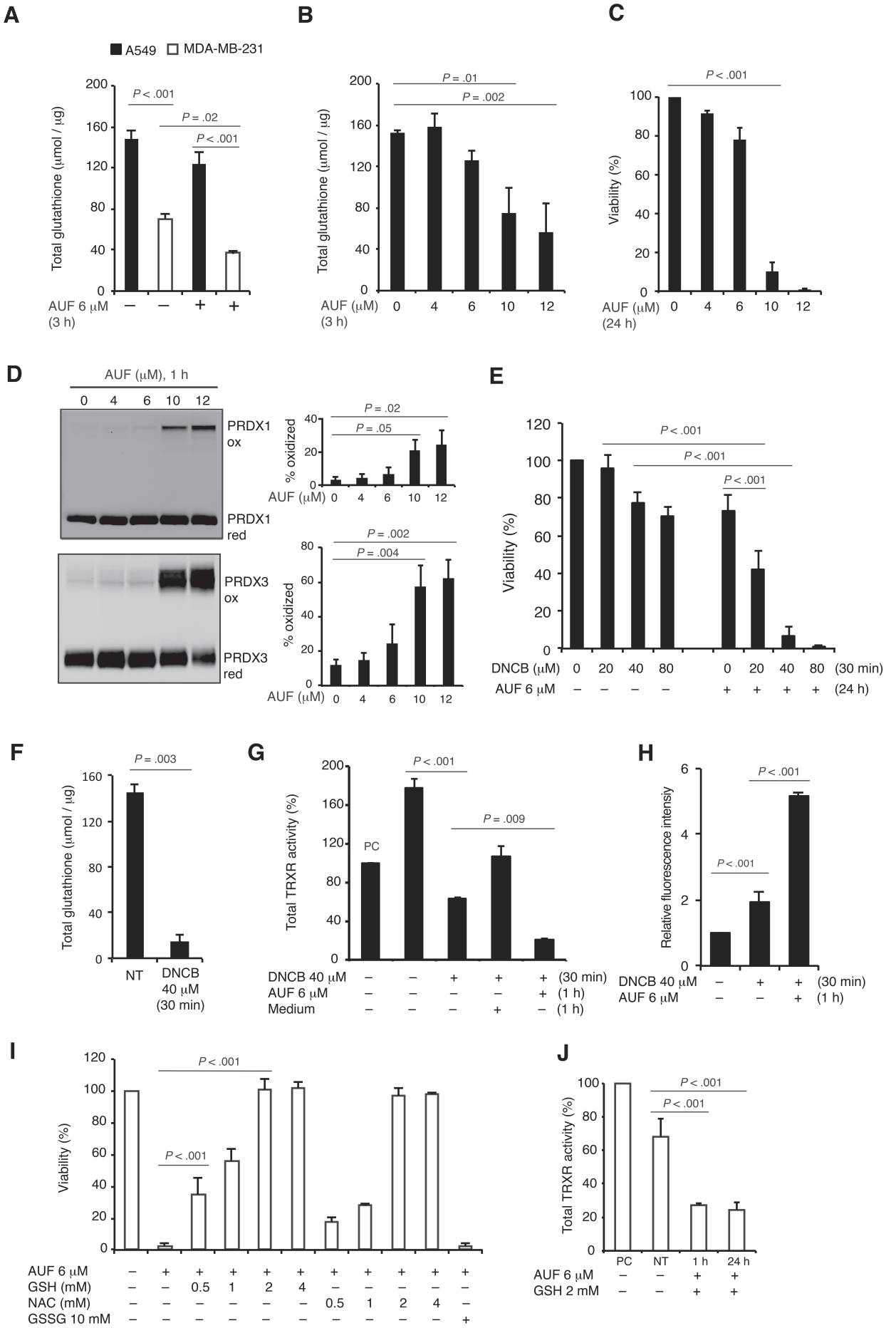
A
A549
MDA-MB-231
Total glutathione (μmol / μg)
P < .001
P = .02
P < .001
AUF 6 μM
(3 h)
B
Total glutathione (μmol / μg)
P = .01
P = .002
AUF (μM)
(3 h)
C
Viability (%)
P < .001
AUF (μM)
(24 h)
D
AUF (μM), 1 h
PRDX1 ox
PRDX1 red
PRDX3 ox
PRDX3 red
% oxidized
P = .02
P = .05
P = .002
P = .004
E
Viability (%)
P < .001
DNCB (μM)
AUF 6 μM
(30 min)
(24 h)
F
Total glutathione (μmol / μg)
P = .003
NT
DNCB 40 μM (30 min)
G
Total TRXR activity (%)
PC
P < .001
P = .009
DNCB 40 μM
AUF 6 μM
Medium
(30 min)
(1 h)
H
Relative fluorescence intensiy
P < .001
DNCB 40 μM
AUF 6 μM
I
Viability (%)
P < .001
AUF 6 μM
GSH (mM)
NAC (mM)
GSSG 10 mM
J
Total TRXR activity (%)
P < .001
PC
NT
1 h
24 h
AUF 6 μM
GSH 2 mM

A

Fractional inhibition and combination index values for AUF/VC combination

AUF (μM)	VC (μM)	Franctional inhibition	Combination index value
1	1000	0.219	0.459
1.5	1500	0.694	0.138
2	2000	0.977	0.021
3	3000	0.979	0.029

B

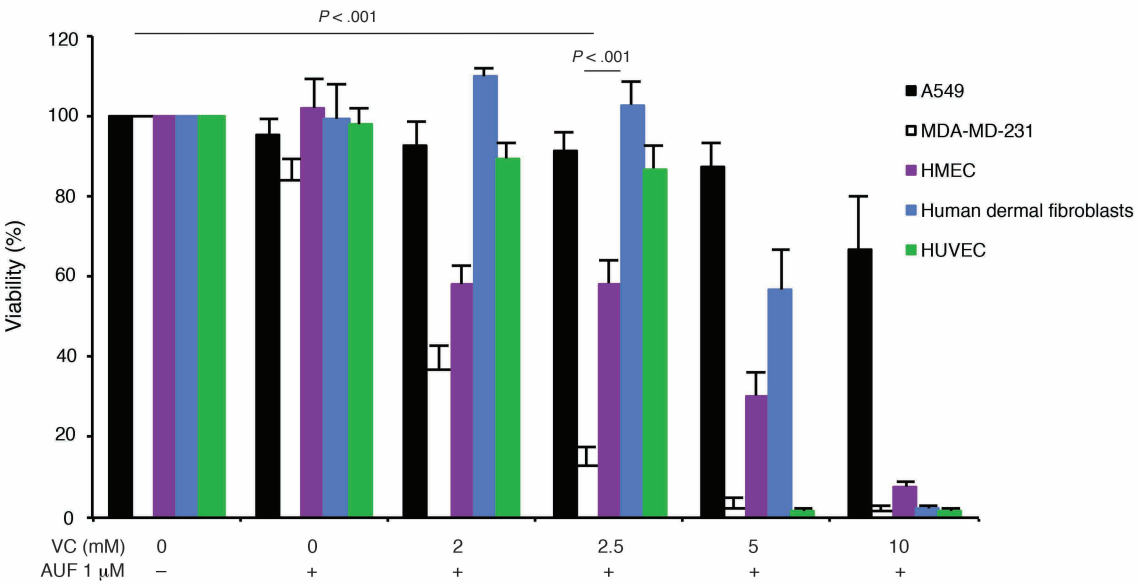

C

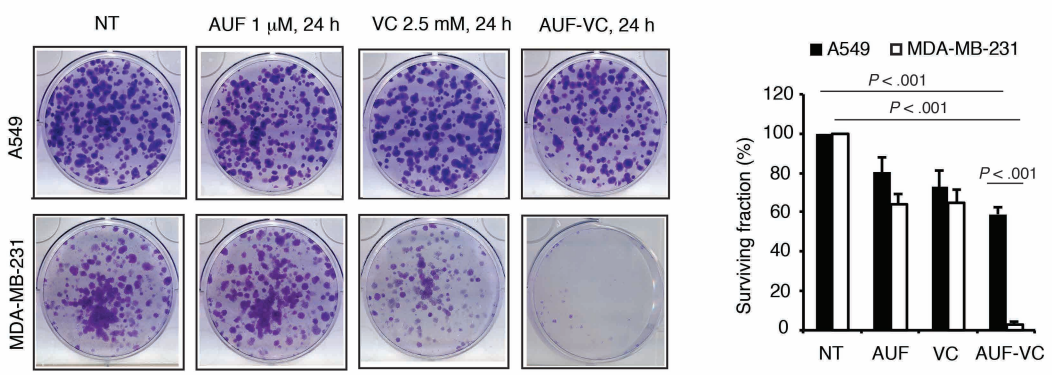

D

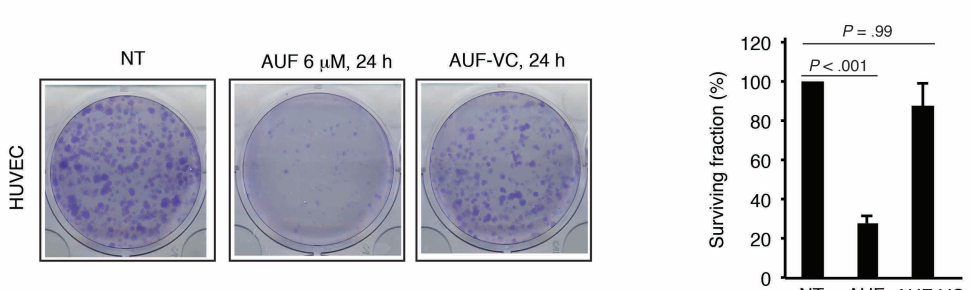

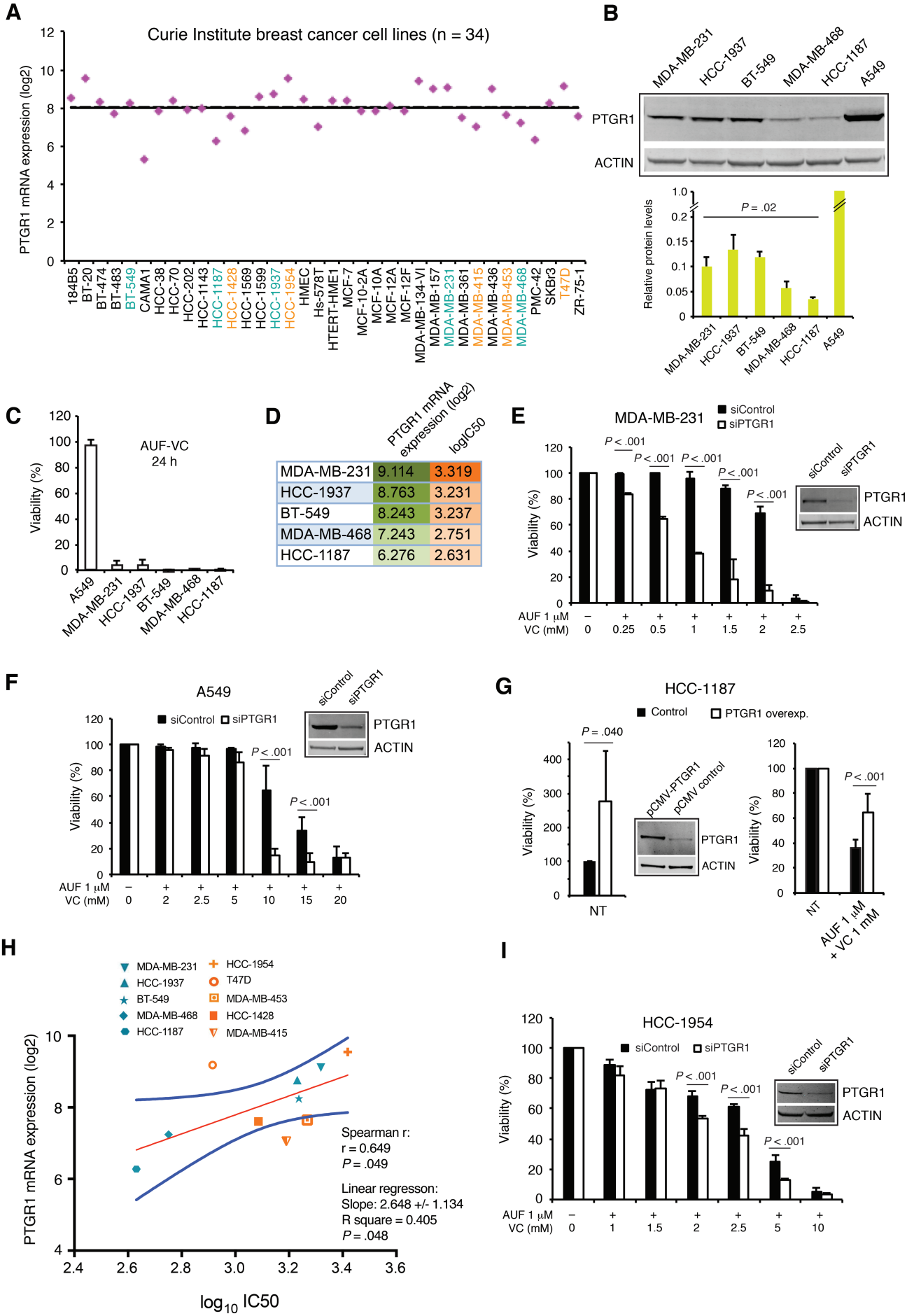
A
Curie Institute breast cancer cell lines (n = 34)
PTGR1 mRNA expression (log2)
184B5
BT-20
BT-474
BT-483
BT-549
CAMA1
HCC-38
HCC-70
HCC-202
HCC-1143
HCC-1187
HCC-1428
HCC-1569
HCC-1599
HCC-1937
HCC-1954
HMEC
Hs-578T
HTERT-HME1
MCF-7
MCF-10-2A
MCF-10A
MCF-12A
MCF-12F
MDA-MB-134-VI
MDA-MB-157
MDA-MB-231
MDA-MB-361
MDA-MB-415
MDA-MB-436
MDA-MB-453
MDA-MB-468
PMC-42
SKBr3
T47D
ZR-75-1
B
MDA-MB-231
HCC-1937
BT-549
MDA-MB-468
HCC-1187
A549
PTGR1
ACTIN
Relative protein levels
P = .02
C
AUF-VC
24 h
Viability (%)
D
PTGR1 mRNA expression (log2)
logIC50
MDA-MB-231 9.114 3.319
HCC-1937 8.763 3.231
BT-549 8.243 3.237
MDA-MB-468 7.243 2.751
HCC-1187 6.276 2.631
E
MDA-MB-231
siControl
siPTGR1
P < .001
Viability (%)
AUF 1 μM
VC (mM)
F
A549
G
HCC-1187
Control
PTGR1 overexp.
P = .040
pCMV-PTGR1
pCMV control
NT
AUF 1 μM + VC 1 mM
H
MDA-MB-231
HCC-1937
BT-549
MDA-MB-468
HCC-1187
HCC-1954
T47D
MDA-MB-453
HCC-1428
MDA-MB-415
Spearman r:
r = 0.649
P = .049
Linear regresson:
Slope: 2.648 +/- 1.134
R square = 0.405
P = .048
log10 IC50
I
HCC-1954

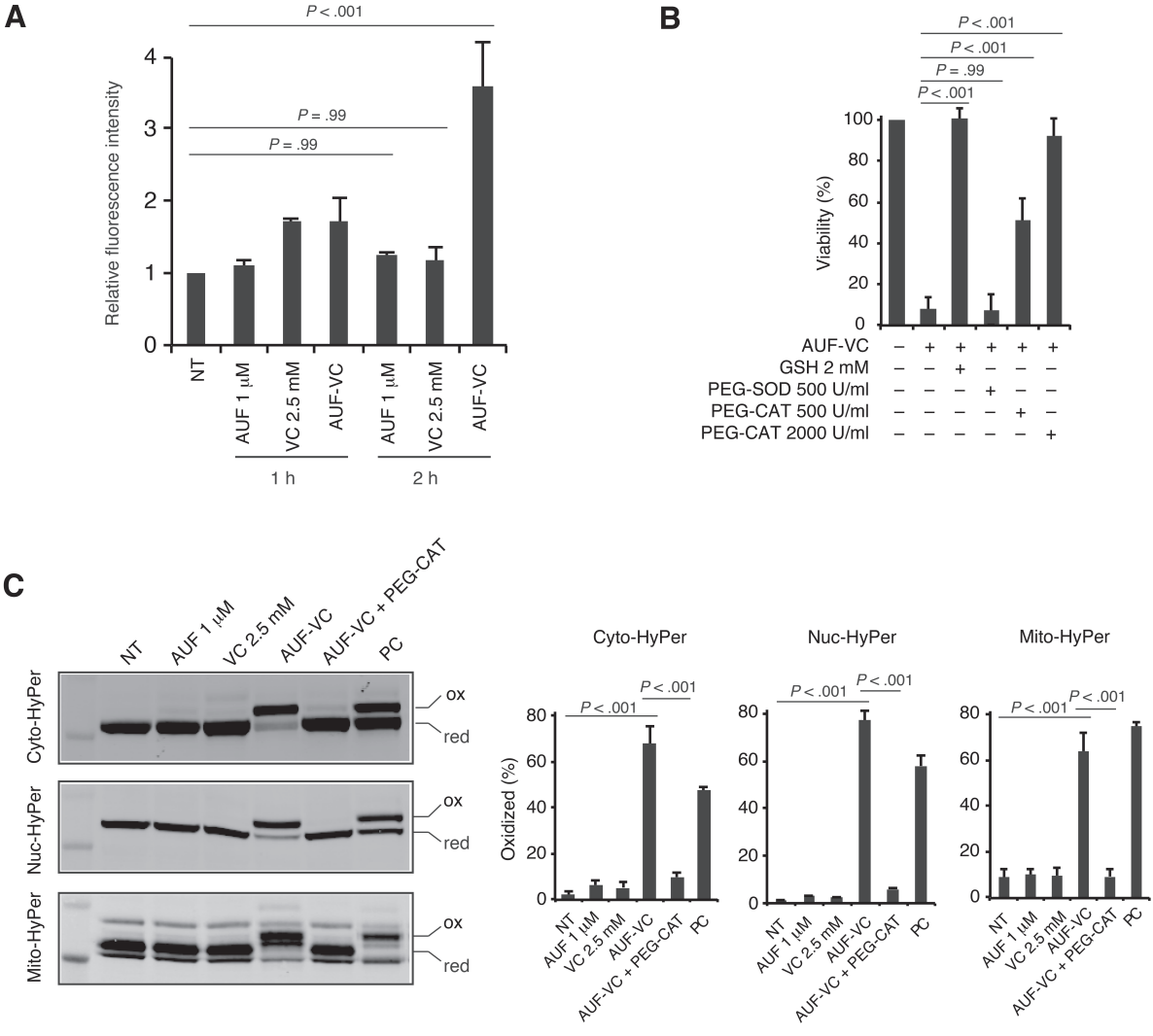
A
P < .001
P = .99
P = .99
Relative fluorescence intensity
0
1
2
3
4
NT
AUF 1 μM
VC 2.5 mM
AUF-VC
AUF 1 μM
VC 2.5 mM
AUF-VC
1 h
2 h
B
P < .001
P < .001
P = .99
P < .001
Viability (%)
0
20
40
60
80
100
AUF-VC – + + + + +
GSH 2 mM – – + – – –
PEG-SOD 500 U/ml – – – + – –
PEG-CAT 500 U/ml – – – – + –
PEG-CAT 2000 U/ml – – – – – +
C
NT
AUF 1 μM
VC 2.5 mM
AUF-VC
AUF-VC + PEG-CAT
PC
Cyto-HyPer
Nuc-HyPer
Mito-HyPer
ox
red
Cyto-HyPer
Nuc-HyPer
Mito-HyPer
Oxidized (%)
P < .001
P < .001
P < .001
P < .001
P < .001
P < .001
0
20
40
60
80
NT
AUF 1 μM
VC 2.5 mM
AUF-VC
AUF-VC + PEG-CAT
PC

A

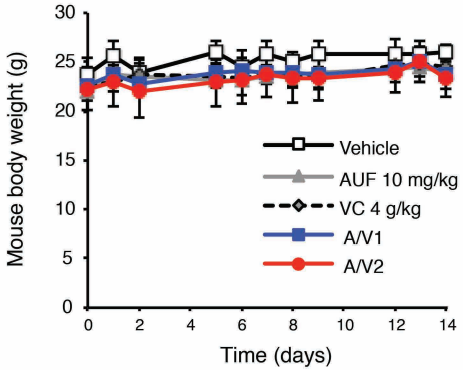

B

Parameter	Vehicle	AUF 10 mk/kg	VC 4 g/kg	A/V1	A/V2
WBC ($\times 10^9$/L)	2.4 ± 0.7	1.5 ± 0.2	1.5 ± 0.3	1.9 ± 0.3	2.6 ± 0.7
LYM (%)	65.8 ± 3.6	63.9 ± 4.2	57.3 ± 14.0	64.6 ± 5.3	66.3 ± 8.5
MON (%)	6.8 ± 1.5	6.3 ± 4.4	9.0 ± 2.2	7.5 ± 3.6	6.9 ± 3.3
NEU (%)	27.4 ± 3.9	29.8 ± 5.2	33.7 ± 12.0	27.9 ± 2.5	26.8 ± 6.3
RBC ($\times 10^{12}$/L)	7.2 ± 0.3	8.0 ± 0.4	7.4 ± 0.4	7.6 ± 0.6	7.4 ± 0.8
MCV(fL)	47.3 ± 5.4	44.7 ± 2.4	45.7 ± 0.9	48.7 ± 1.9	46.3 ± 0.5

A/V1: AUF 5 mg/kg + VC 4 g/Kg
A/V2: AUF 10 mg/kg + VC 4 g/Kg

C

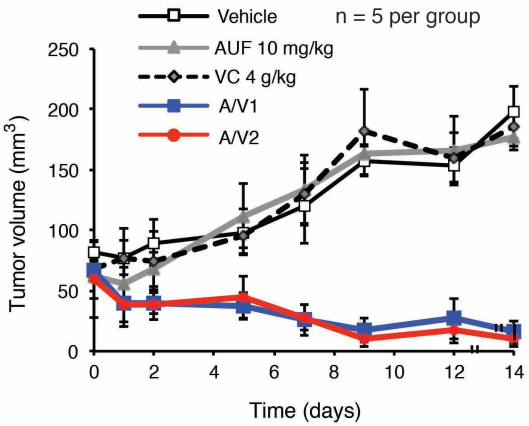

D

	Group	Tumor volume (mm^3) mean ± SD	Adjusted *P* value*
Day 0	Vehicle	82.11 ± 8.99	
	AUF 10 mg/kg	61.62 ± 17.83	0.31
	VC 4 g/kg	71.59 ± 6.63	0.83
	A/V1	66.68 ± 9.52	0.56
	A/V2	59.94 ± 31.72	0.23
Day 14	Vehicle	197.67 ± 24.28	
	AUF 10 mg/kg	176.72 ± 11.50	0.29
	VC 4 g/kg	182.30 ± 17.52	0.57
	A/V1	15.66 ± 10.90	< 0.001
	A/V2	10.23 ± 7.30	< 0.001

* adjusted *P* values for the difference in tumor volume between vehicle and indicated groups

E